A Numerical Study of Circulations Induced by a Dry Salt Lake

W. L. PHYSICK

CSIRO Division of Atmospheric Research, Aspendale, Victoria, Australia

N. J. TAPPER

Department of Geography and Environmental Science, Monash University, Clayton, Victoria, Australia

(Manuscript received 5 July 1989, in final form 13 November 1989)

ABSTRACT

Observations of surface winds in the vicinity of a moderate-sized (about 70 km^2) dry salt lake by Tapper suggest that differences in albedo and soil thermal properties between the salt and surrounding sand surfaces may be strong enough to drive a mesoscale thermal circulation. In this paper a numerical mesoscale model is used to investigate disturbances generated by moderate and large-sized (about 7000 km^2) lakes. In the latter case, a typical size for the great salt lakes of inland Australia, disturbances with strong horizontal and vertical shear are found at a distance of more than 200 km from the lakeshore by midnight. The separate contribution of albedo and soil property differences to the circulation are assessed, under both dry and moist soil conditions. The possible influence of such circulations on regional climate is discussed and it is suggested that salt lakes may be a source for solitary waves observed in the Australian interior.

1. Introduction

Atmospheric circulations arise from horizontal pressure gradients associated with adjacent air masses of different temperature. On the mesoscale, a horizontal variation in sensible heat flux from the ground is responsible for many such systems. Perhaps the best-known example is the sea- and land-breeze circulation in which the differential flux of sensible heat arises from the significantly greater heat capacity of water when compared to land.

In recent years there has been considerable interest in circulations that develop completely over land, where a difference in soil moisture availability between adjacent areas is responsible for the differential sensible heat flux. In this situation the amount of energy available for partitioning between sensible and latent heat is approximately the same at each surface, but the moister area uses more energy in evaporative processes than the drier, and consequently has less available for sensible heat.

Ookouchi et al. (1984) numerically studied this type of circulation over bare soil and found it can be as strong as a sea breeze, as did Yan and Anthes (1988) who included cloud and precipitation schemes in their simulations. Assuming the moister surfaces corresponded to areas of vegetation, the latter authors were able to support the hypothesis of Anthes (1984) that planting of bands of vegetation of order 100 km wide in semiarid regions could produce increases in convective precipitation when large-scale conditions were favorable. Using a mesoscale model with a vegetation module, Mahfouf et al. (1987) showed that a total vegetative cover over a region of varying soil moisture can considerably reduce the differential heat flux and circulation strength from that obtained in the bare soil case. Circulations induced by adjacent vegetated and bare soil areas, and comparable in strength to sea breezes, were obtained under certain favorable conditions by Segal et al. (1988). However, for conditions more typical of real-world situations, involving evapotranspiration rates and density of vegetative cover, the resulting circulations decreased in intensity.

Observations by Tapper (1988, 1990) suggest that the difference in sensible heat flux arising from the differing albedo and soil thermal conductivity and diffusivity values of neighboring areas may also be sufficient to induce a circulation. These data were obtained in the vicinity of a dry salt lake in Australia and are presented in section 2. A higher albedo value for the lake than for the surrounding sand, and a higher thermal conductivity and diffusivity beneath the salt surface mean that less energy is available over the salt lake for partitioning into sensible and latent heat. The aim of this paper is to use a numerical model to investigate the findings of Tapper (1988, 1990) further, and to assess the relative contributions of albedo and conductivity/diffusivity differences to the circulation. The importance of salt-lake size is also discussed. The me-

Corresponding author address: Dr. William L. Physick, CSIRO Division of Atmospheric Research, Private Bag No. 1, Mordialloc, Victoria 3195, Australia.

soscale model and experiments are described in section 3, with results and discussion following in sections 4 and 5.

2. Observations

The location and dimensions of the lake, known as The Salt Lake, are shown in Fig. 1. Situated approximately 1000 km northwest of Melbourne in an eastern extension of the Strzelecki dune fields, The Salt Lake is one of the most accessible salt pans of reasonable size in the Australian arid zone. It is perennially dry, filling perhaps once every 10 years, and then only for a few months. Details of the lake environment and the experiments carried out in April 1985, October 1985, and April 1986 can be found in Tapper (1990). For the purposes of this paper, only observations from April 1985 and 1986 are discussed. A time series of surface divergence for the period 21–23 April 1986, computed from a network of 6 anemographs located around the lakeshore (Fig. 2), suggests the existence of a circulation of diurnal period, probably arising from different heating rates over the salt surface and the surrounding sand dunes.

Upper winds on 21 and 22 April 1986 were obtained from pilot balloons released at approximately two-hourly intervals from a lakeshore site indicated in Fig. 1. These also suggest a shallow circulation, extending to no more than 400 m, imposed on a 3–4 m s^{-1} westerly synoptic wind (Fig. 3). An unusual aspect of the system is the replacement of the onshore flow by offshore westerlies in midafternoon for a few hours, fol-

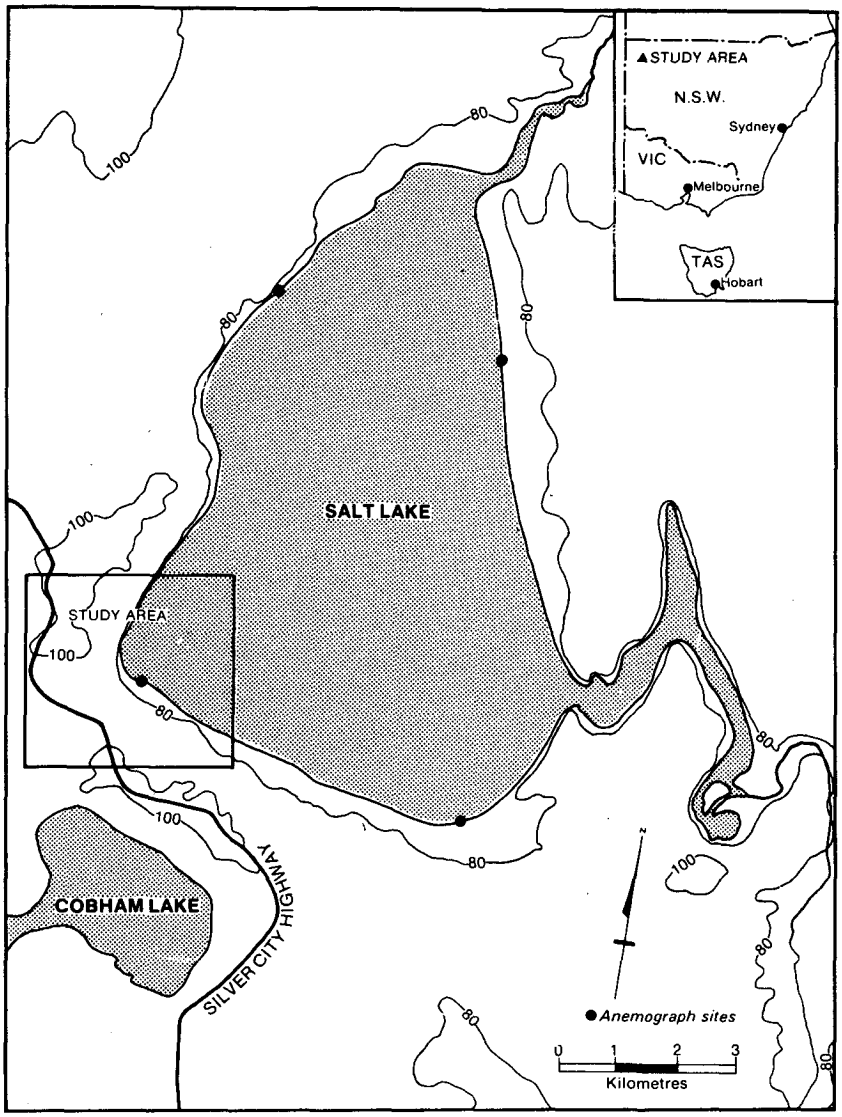

FIG. 1. The Salt Lake geometry and location. Contours indicate elevation above mean sea level in meters.

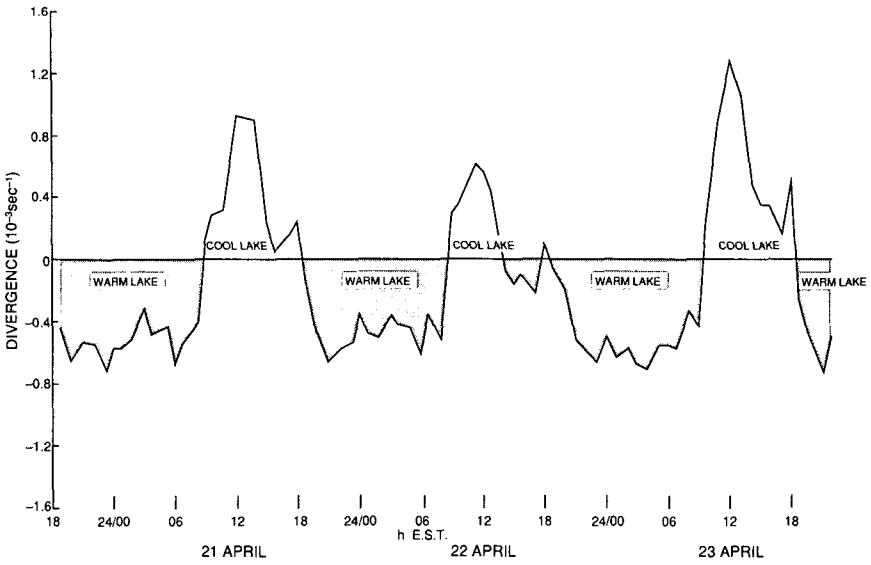

FIG. 2. Surface divergence at The Salt Lake, 21–23 April 1986, computed from anemographs.

lowed by a return to onshore winds around 1700 EST. All low-level winds are light, and convective mixing of higher-level westerlies to lower levels in the afternoon followed by the decay of convection a few hours later may be responsible for the changing wind directions. This midafternoon disruption of the lake-breeze circulation appears to occur on a daily basis during the period 21–23 April (Fig. 2). Toward 2000 EST, the flow switches to offshore, presumably in response to greater cooling over the sand dunes than over the salt surface.

Radiant surface temperature and albedo were obtained from field traverses across the region. Data from midafternoon and early-morning traverses on 22–23 April 1985 are presented in Fig. 4. Albedo is determined from the ratio of outgoing and incoming solar irradiance, spectrally integrated from 0.3–3.0 μm, using upward facing and inverted pyranometers. Surface temperatures differ by about 15°C during the daytime, while at night the gradient reverses sign, with a difference of about 5°C between salt and sand. Albedo of the dry salt crust (0.6) is twice that of the sand surface.

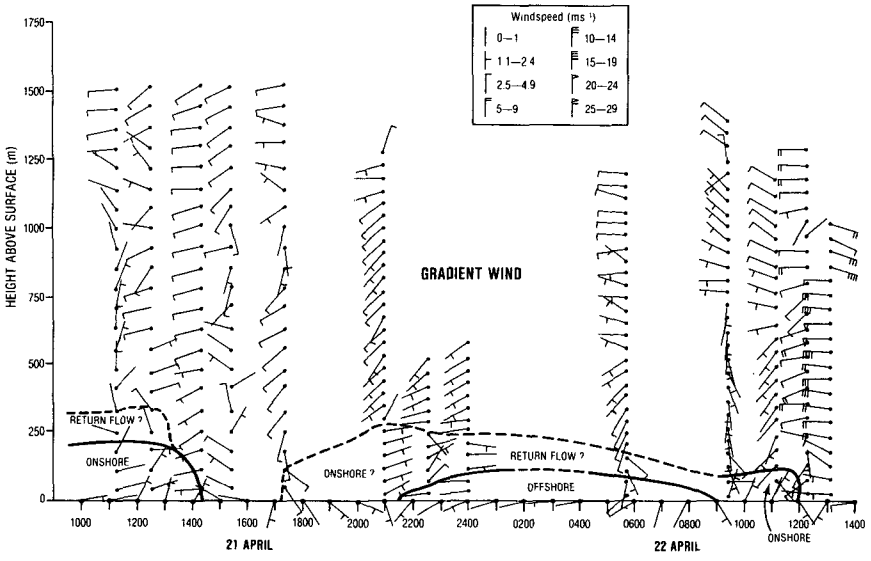

FIG. 3. Time–height section of airflow on the western margin of The Salt Lake, 21–22 April 1986. (Air layers have been subjectively discriminated.)

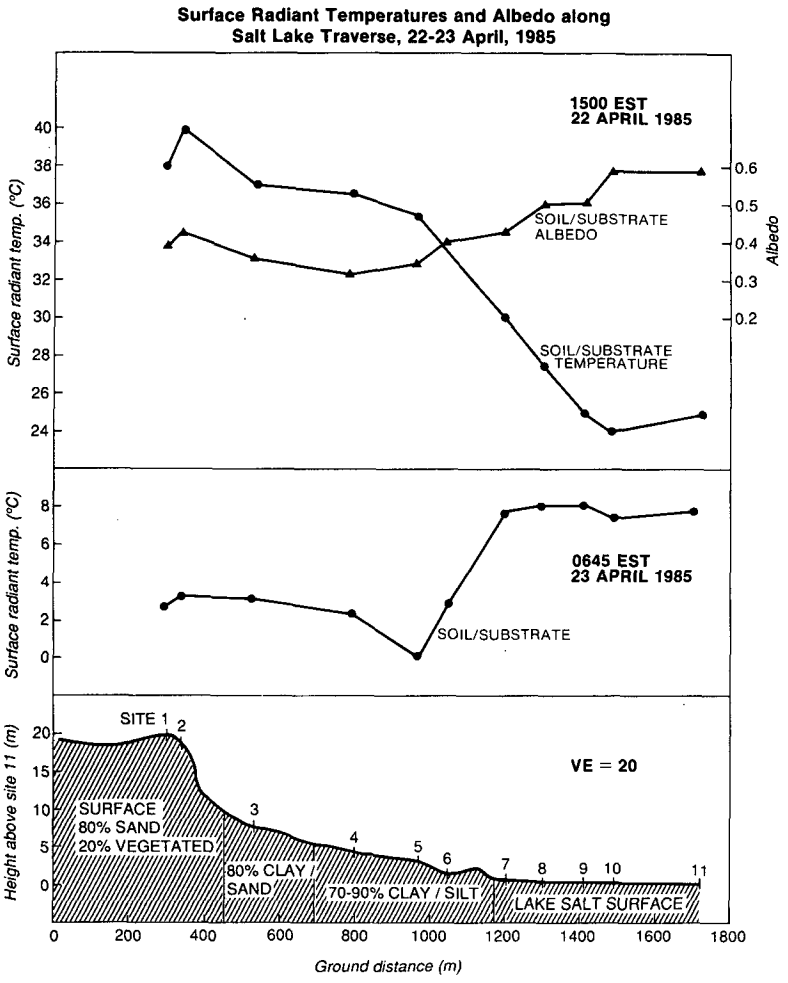

FIG. 4. Radiant surface temperatures and albedo across The Salt Lake region, at 1500 EST 22 April and 0645 EST 23 April 1985.

Temperature at levels 1, 10, 30, and 75 cm in the soil were also obtained at sand and salt sites. Values are presented in the following sections when discussing the numerical experiments.

3. Numerical model and experiments

The Colorado State University mesoscale model (Mahrer and Pielke 1977; McNider and Pielke 1981) is used in this study in a three-dimensional mode. It is hydrostatic, incompressible, and includes a detailed planetary boundary layer scheme in which surface temperature is calculated from energy-balance considerations. Surface fluxes of momentum, heat, and moisture are calculated from Monin–Obukhov similarity theory, while soil heat flux is calculated by solving the thermal diffusion equation at 15 levels in the soil, spaced 5 cm apart. Data show that the diurnal temperature wave does not penetrate as deep as 75 cm below either surface.

Values of soil thermal conductivity and diffusivity used in the model were calculated from the observed temperatures in the sand and salt soils. These, and albedo values from Fig. 4, can be found in Table 1, and are consistent with the observation that surface temperatures are higher on the sand dunes than on The Salt Lake during the daytime, with the opposite being the situation at night. The relative contribution of the albedo and soil thermal properties to lake-induced flow perturbations is assessed in section 4.

Field experiments indicated very little evaporation over both sand and salt (0–30 W m^{-2}), indicating that nonuniform horizontal distribution of surface moisture was not a factor in the generation of the circulation. Consequently, the soil moisture availability parameter in the model, denoted as m was set to 0.01 [this is defined as the ratio of the surface evaporation rate to the potential (saturated) evaporation rate]. This results in a Bowen ratio of about 14 for a few hours either side of midday. Surface humidity is calculated from

the sum of saturated surface humidity and humidity of the first model level (2 m), weighted by m and $1 - m$ respectively.

Observations showed that surface temperatures over sand and salt were equal (17.7°C) at 0850 EST. Model runs were commenced at this time with the observed soil temperature profiles shown in Fig. 5.

In the absence of data the initial potential temperature profile in the atmosphere was specified in the following manner. A mixed layer of 290.7 K to a height of 145 m was capped by a layer of stability 2 K km^{-1} to 1750 m, representing the slightly stable remains of the previous day's mixed layer. Above this height, a lapse rate of 4 K km^{-1} to the model top of 6500 m was assumed. A representative geostrophic wind, obtained from Fig. 3, of 3.5 m s^{-1} from the west was imposed.

Runs were carried out on a $40 \times 40 \times 16$ grid with a horizontal grid spacing of 1 km, and in later experiments 10 km. The location of The Salt Lake is indicated in the illustrations of the following section and flat terrain was assumed (the maximum variation in relief within a 30 km radius of The Salt Lake is in fact less than 25 m). Spacing in the vertical was variable, with finer resolution near the surface and the first model level at 2 m above the ground. Further levels used are 10, 30, 90, 200, 350, 550, 800, 1100, 1500, 2000, 2700, 3500 m and 3 additional levels spaced 1000 m apart to 6500 m. A value of 0.005 m was used for the roughness length z_0.

Details of experiments performed can be found in Table 1. First, a run with a horizontal grid spacing of 1 km is carried out to simulate The Salt Lake conditions. The relatively small domain limits the simulation time for this run (see section 4.1), and further runs with a lake of identical geometry but 10 times the size of The Salt Lake (and a ten-fold larger domain) are also carried out. Within this latter series of runs, the influence of synoptic wind (zero versus nonzero), albedo, and soil thermal properties is investigated.

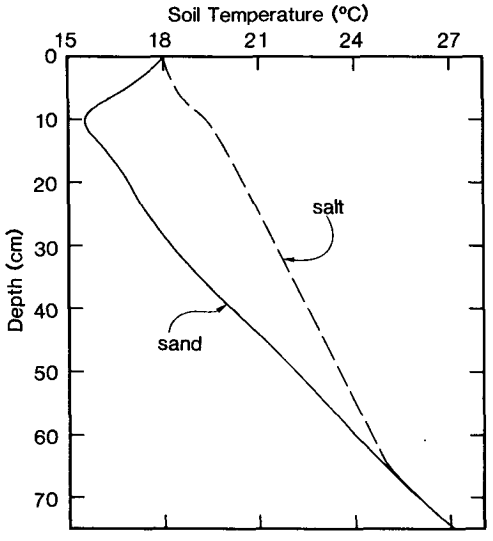

FIG. 5. Initial soil temperature profiles in sand and salt, based on observations.

4. Results

a. *Small lake (run 1)*

The numerical results confirm the suggestion from the data that thermal effects from a dry salt lake of roughly 4 km radius cause a significant perturbation to the synoptic flow. This disturbance is advected downwind of the lake and reaches the domain boundaries (about 25 km from the shoreline) after 4 hours simulation time. Subsequently, partial reflection from the boundaries (where zero-gradient boundary conditions are employed) gradually contaminates the solution throughout the domain.

The nature of the disturbance at 1200 LST (all model results are LST) is illustrated in Fig. 6. Over the lake, winds at 10 m (Fig. 6a) are generally reduced in magnitude from the upstream value as they respond to the horizontal pressure gradient arising from the cool lake and warmer sand, although the temperature difference is only 1.7 K at a height of 6 m, decreasing to 0.3 K at 950 m. Windshift lines downstream of the lake are also evident in Fig. 6a. Stronger winds are found behind these weak mesoscale fronts with a north–south temperature difference of only 0.6 K at low levels near the eastern boundary. A horizontal cross-section (at 350 m) of the vertical velocity field, which is evident to about 2000 m, shows narrow regions of upward motion at the leading edge of the windshift lines and a broader subsidence region downwind of the lake (Fig. 6b).

Agreement between the morning pibal winds of Fig. 3 and the numerical results is not good. For example, onshore winds observed to a height of 200 m, do not eventuate in the model (southwesterly corner of the lake) although the strength of the synoptic offshore westerlies does decrease significantly. The discrepancy may arise from incorrect specification of the initial wind field, due perhaps to variation of the geostrophic wind with height or to local mesoscale winds related to nocturnal lake effects. However, the simulation has suggested some significant effects can be induced by a relatively small salt lake, including the downstream propagation of windshift lines in light to moderate synoptic wind conditions. The associated updrafts at the leading edges and large subsidence regions behind may also have implications for regional climate. These are discussed further in section 5.

b. *Larger lake with nonzero synoptic wind (run 2)*

There are more than 200 dry salt lakes the size of The Salt Lake or larger in the Australian landscape, including approximately 20 with at least one dimension

TABLE 1. Parameter values assigned for the five simulations discussed in this paper.

Run no.	Grid spacing (km)	Synoptic wind ($m\ s^{-1}$)	Albedo		Diffusivity ($m^2\ s^{-1} \times 10^{-6}$)		Conductivity ($W\ m^{-1}\ K^{-1}$)	
			Sand	Salt	Sand	Salt	Sand	Salt
1	1	3.5 from west	0.3	0.6	0.26	0.83	0.31	2.57
2	10	3.5 from west	0.3	0.6	0.26	0.83	0.31	2.57
3	10	zero	0.3	0.6	0.26	0.83	0.31	2.57
4	10	zero	0.3	0.3	0.26	0.83	0.31	2.57
5	10	zero	0.3	0.6	0.26	0.26	0.31	0.31

in the order of 60–80 km. The two largest, Lake Eyre North and Lake Mackay, are at least this size in both north–south and east–west directions. Thus, in light of the previous section's findings, it may be interesting to examine the mesoscale flow perturbations associated with salt lakes of these dimensions. This is done here by using a grid spacing of 10 km, but keeping all other parameter values the same as for the small lake, including the number of grid points and the lake geometry. This means the lake is now of order 70 km across and the domain is 390 × 390 km. Starting time is 0850 LST and the synoptic wind is again 3.5 m s^{-1} from the west.

As the duration of this run is not limited by lateral boundaries it is possible to examine the diurnal temperature variations of both sand and salt surfaces and compare the variations with the data from The Salt Lake. Values from grid points just onshore and offshore, (6, 18) and (7, 18), are shown with the observations in Fig. 7. Modeled temperatures reflect the diurnal pattern observed at both sand and salt surfaces, although the amplitude of the salt surface wave is a few degrees larger than recorded. It is interesting to note that the relatively small diurnal temperature wave observed at the salt surface is usually associated with highly wet soil. However, even though the salt crust (about 2 cm deep) is dry and exhibits very little evaporation, the fine clay/silt particles comprising the sediments beneath are virtually saturated, resulting in a thermal conductivity and diffusivity that are 50%–100% larger than other "typical" wet soils [e.g., see Table 2.1 in Oke (1987)]. The relatively high albedo of the dry salt crust, when compared to soils, also contributes to the small temperature wave.

Winds at 10 m at 1400 LST are shown in Fig. 8a. The lake causes a strong perturbation to the synoptic flow in the form of very light winds over much of the salt surface and enhanced winds for about 60 km downwind of the eastern shoreline. Comparison with 10 m winds for the smaller lake (Fig. 6a) shows qualitative similarities, although with a Rossby number of order 1 a simple "scaling up" of results from the smaller lake to a larger one is not valid.

Maximum vertical velocities occur at about a height of 1000 m, with subsidence (−11.5 cm s^{-1}) almost twice as strong as the upward motion (+6.8 cm s^{-1}) at the leading edge of the windshift lines (Fig. 8b). The larger vertical velocities in the smaller lake simulation (Fig. 6b) are due to the smaller horizontal gridlength employed in that run. Subsidence over the lake is consistent with the observations of Strong (1972) who evaluated the effect of Lake Michigan (width 126 km), during spring, on the synoptic flow. Downward motion during the daytime was observed over the lake at all times, whether the prevailing gradient wind was onshore, offshore, or parallel to the shore. Lyons (1972) also presents further evidence in the form of a satellite photo showing cloud-free regions over the Great Lakes, while cumulus clouds are evident over the surrounding land areas.

A vertical cross-section through the southern part of the lake (Fig. 8c) reveals shear associated with the disturbance extending to about 2000 m, while the temperature difference of less than 1.5 K across this wind system (Fig. 8d) is quite small when compared with sea breezes.

While a priori one might expect that a disturbance generated by a fairly weak thermal differential in the horizontal would decay soon after sunset when temperature gradients reverse sign across the shoreline, inspection of the wind fields at 2200 LST (Fig. 9) shows that this is not the case. Indeed, the maximum wind speeds at this time are stronger than daytime values due to smaller friction forces at night (Physick 1976), and are situated about 200 km east of the lakeshore (Fig. 9c). Similar nocturnal disturbances in subtropical Australia have been observed and modeled previously (e.g., Clarke 1983; Physick and Smith 1985) but these are generated at the northeastern Australia coastline where temperature differentials are typically 8 K and the ocean provides a vast supply of cool air. Further discussion on the relevance of the model results to these and other disturbances observed in inland Australia is reserved until the next section.

An aspect of these nocturnal flow fields that may be important for light aviation is the location of the regions of strong horizontal shear. The region of maximum shear tilts strongly between the surface (Fig. 9a) and the 1500 m level (Fig. 9d) and is located between 70 and 100 km from the lake. Over the lake itself there is

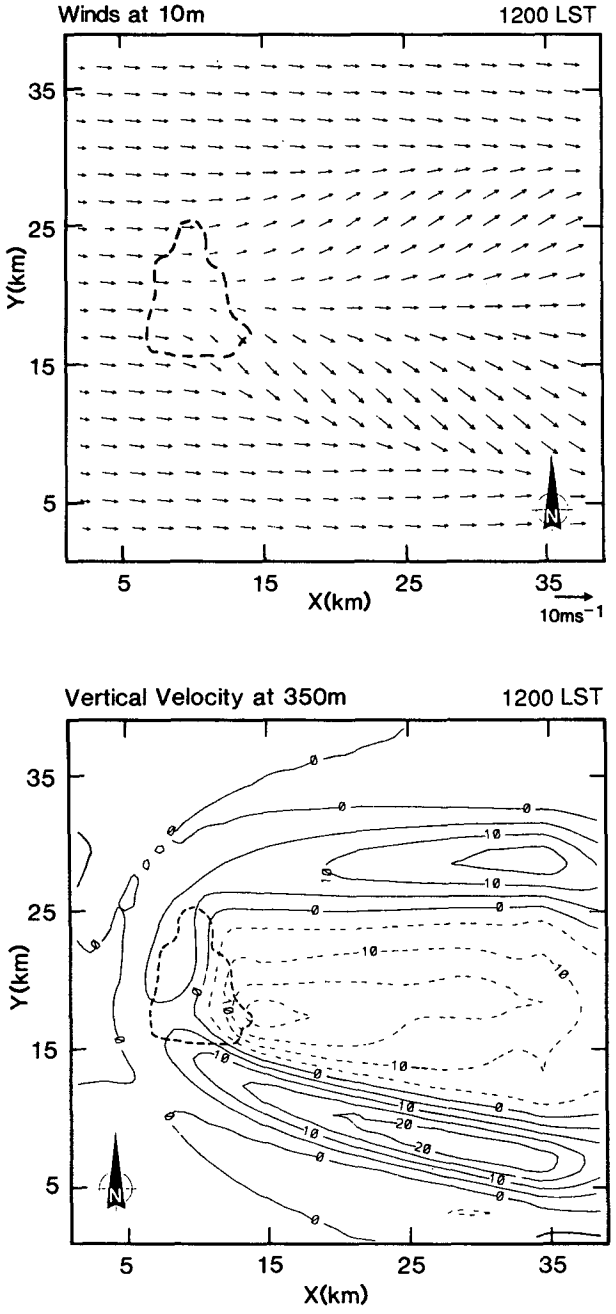

FIG. 6. Horizontal cross-sections at 1200 LST of (a) winds at 10 m, and (b) vertical velocity at 350 m (contour interval 5 cm s^{-1}) for the small-lake simulation (Δx = 1 km). Dashed contours indicate negative values.

little perturbation of the synoptic flow field above 800 m (Figs. 9c,d).

c. *Larger lake with zero synoptic wind (run 3)*

The mesoscale wind system induced by the salt lake under zero synoptic wind conditions differs considerably from that of the previous section. The disturbance is centered on the lake and does not extend as far from the lakeshore. By 1600 LST, onshore winds of about 3 m s^{-1} strength and depth 500 m extend radially from the lake center for a distance of 20 km (Fig. 10a). As with the nonzero case (Fig. 8b), rising motion exists at a circular windshift line, with a subsidence region behind, with the associated temperature fall being less than 2 K.

After sunset, the wind system moves away from the shoreline at a faster rate, due to the reduction of frictional forces, and by midnight the leading edge is about 80 km from the lake (Fig. 10b). Winds have become almost parallel to the shoreline by this time, due to Coriolis turning, and the system becomes stationary and weakens until only very light winds exist near the surface by 0600 LST. Note that a vortex-like pattern similar to Fig. 10b, but in an opposite sense (inflow instead of outflow) exists at higher levels between 1000 and 2000 m. This is a direct consequence of Coriolis turning of the return flow of the circulation.

In order to compare this nonclassical mesoscale circulation with a sea-breeze circulation (or strictly speaking a lake-breeze circulation), a run was carried out in which the temperature of the salt surface was kept constant throughout at its initial (0850 LST) value of 17.7°C. In general, maximum vertical velocities were 50% larger in the sea-breeze run and horizontal winds were twice as strong.

d. *Contributions of albedo and soil thermal properties to the circulation*

Two further runs were performed for the larger lake (Δx = 10 km) with zero synoptic wind. Comparison

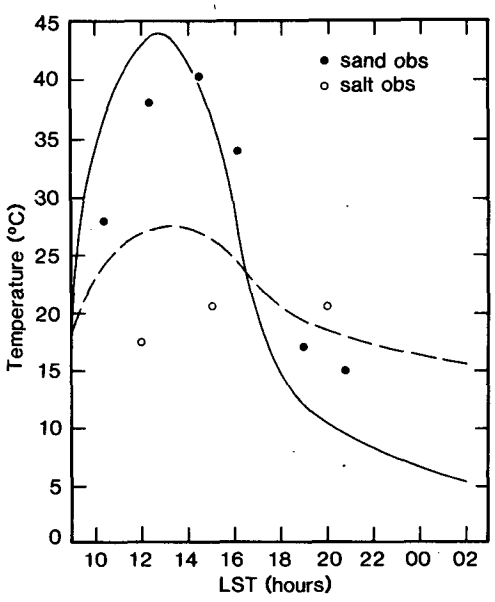

FIG. 7. Modeled diurnal variation of surface temperature at sand (solid) and salt (dashed) grid points. Also shown are observations from The Salt Lake.

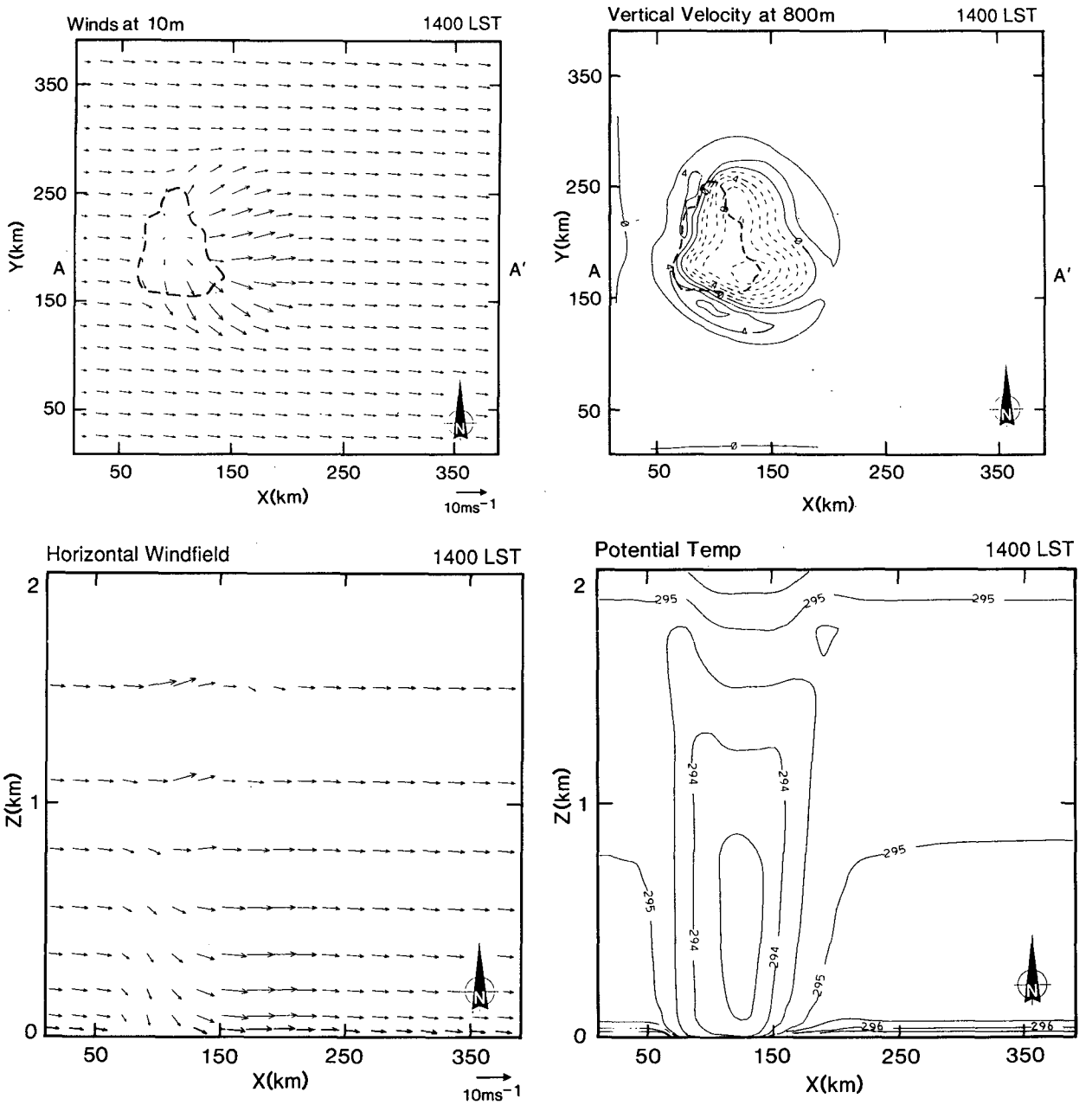

FIG. 8. Modeled fields at 1400 LST for the large-lake simulation (Δx = 10 km) with synoptic wind of 3.5 m s^{-1} from 270 degrees. (a) Horizontal cross section of the winds at 10 m; (b) horizontal cross-section of vertical velocity at 800 m, contour interval 2 cm s^{-1} and dashed contours indicate negative values; (c) vertical cross section through AA^1 [see 8(a)] of the horizontal windfield; vectors pointing to the right indicate westerly flow and arrows pointing downward indicate northerly flow; (d) vertical cross section through AA^1 of potential temperature, contour interval 0.5 K.

of these with the results of section 4c enabled an assessment of the separate contributions of albedo and soil thermal properties to the circulation. Run 4 evaluated the soil property difference (albedos of both surfaces set to the sand value) and run 5 examined albedo differences (soil properties set to the sand value).

Up until midday, the relative influence of both parameters on the circulation was about the same, as can be seen from Table 2 in which values of various indicators for each run are listed. Also shown are values from the run discussed in section 4c, in which both influences are simulated, indicating that the combined effect cannot be estimated by simply adding individual contributions. The albedo-induced circulation continues to strengthen throughout the day while the conductivity/diffusivity perturbation weakens from mid-

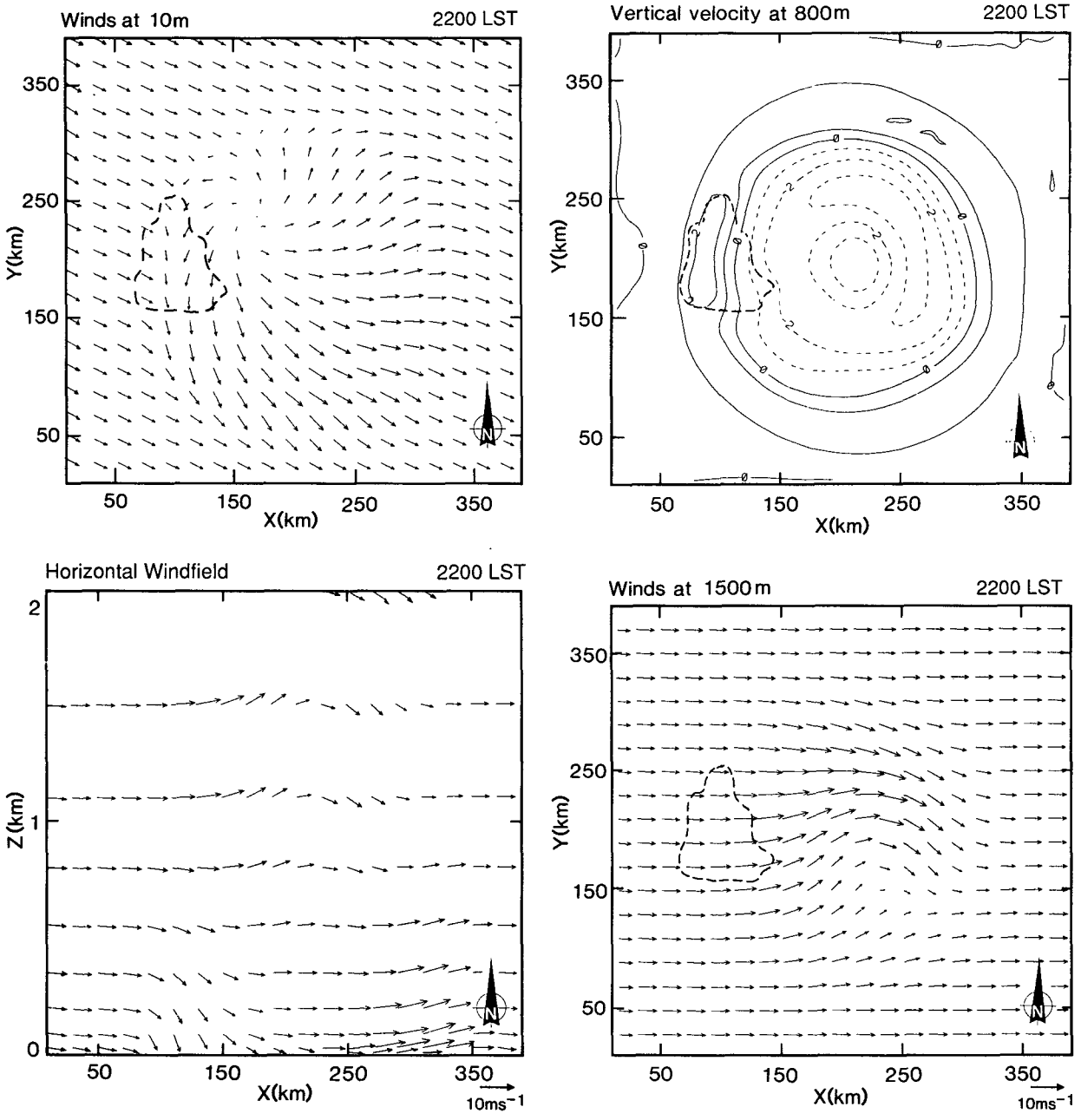

FIG. 9. As in Figs. 8(a)–(c) but at 2200 LST. (d) Horizontal cross section of winds at 1500 m. Note that contour interval in 9(b) is 1 cm s^{-1}.

afternoon when downwards heat flux to the deep soil below the salt surface weakens and sensible heat fluxes over both surfaces are close to the same value.

After sunset, the soil property-induced circulation continues to weaken rapidly as heat flows upwards from the deep soil to the salt surface at a faster rate than it does to the sand surface, thus reducing and eventually reversing the temperature gradient in the lower layers of the atmosphere. However, this process does not occur when the lake breeze arises purely from albedo differences and the circulation remains relatively strong after sunset, eventually decaying in the manner described by Clarke (1984) and Physick and Smith (1985) for sea breezes. Examination of Fig. 10b and Fig. 11 shows that the maintenance of the salt-lake circulation until at least 2400 LST can be attributed to the difference in albedo between the sand and salt rather than to differences in soil thermal properties.

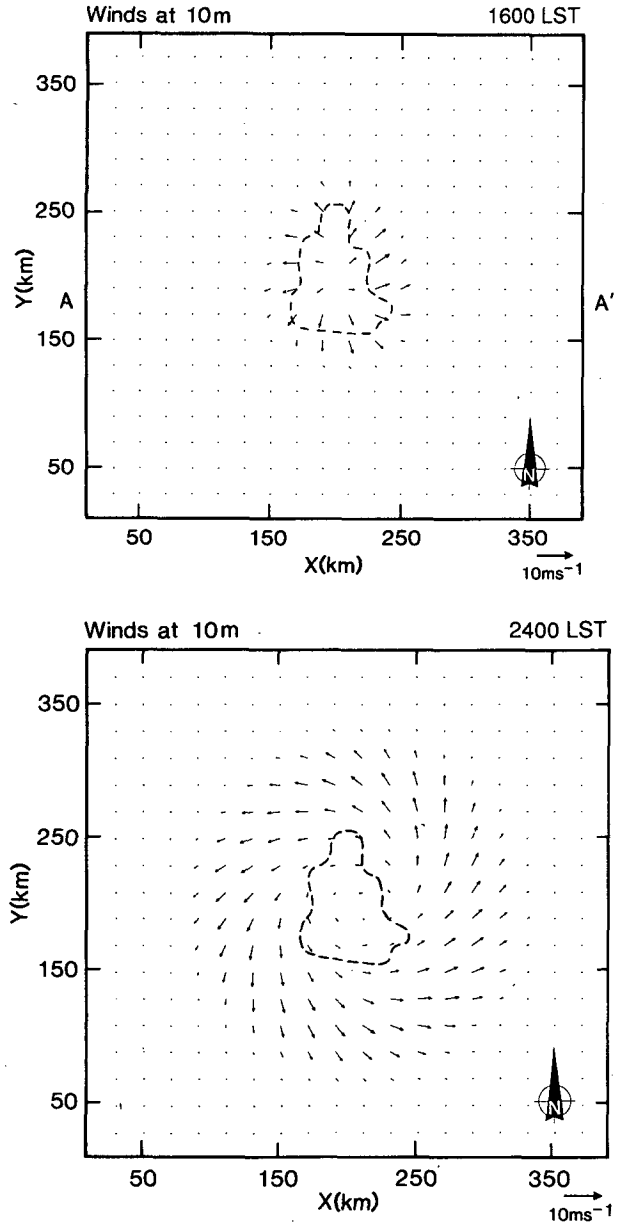

FIG. 10. Horizontal cross section of winds at 10 m for the large-lake simulation ($\Delta x = 10$ km) for zero synoptic wind. (a) 1600 LST, (b) 2400 LST.

e. *Dependence of circulation strength on soil moisture*

Although we are primarily concerned in this paper with the *dry* salt lakes of Australia, it may be of interest to briefly examine the relation between soil moisture and the strength of the circulation. This is especially so in light of the findings of Mahrer and Pielke (1978) who found that an albedo-induced circulation across two completely dry regions virtually disappeared when a little moisture (5%) was present at the lower-albedo surface.

The relative circulation strengths under different conditions can be examined by performing a series of one-dimensional experiments. The circulation intensity at any time is proportional to the difference in the time-integrated heat input (sensible heat flux) over the salt and sand surfaces (e.g., see Pearson 1973). Figure 12a shows the time behavior of these flux differences, calculated from one-dimensional integrations for the three zero-wind experiments of the previous sections. Broad conclusions from Fig. 12a are consistent with the findings of section 4d, namely that up until midday the influences of albedo and soil property differences are about the same, but after this time the circulation arising from soil-property differences weakens relative to the albedo-induced circulation. For comparison purposes, the differential heat input by 1700 LST for the sea-breeze run of section 4c (constant salt-surface temperature) is 1773 W m^{-2}.

The effect of soil moisture on the circulations can be inferred from Fig. 12b, which shows the same experiments as Fig. 12a except with the value of the soil moisture availability parameter m set to 0.2 for both surfaces. This value of m gives a Bowen ratio of 0.9 in the middle of the day. All circulations have decreased in intensity, due to less available energy being partitioned into sensible heat than previously, but not all to the same extent. Circulations arising from soil-property differences are reduced more by the presence of soil moisture than those induced by different albedos. This occurs because, in the latter case sensible heat fluxes are reduced by the same percentage over both surfaces, whereas in the former there is a greater percentage reduction of fluxes over the poorer conducting (and higher temperature) surface than over the better conductor.

We have also examined the situation where the two soils contain differing amounts of moisture. Figure 13a shows the heat input difference as a function of m for two surfaces of differing albedo, but the same soil properties. The higher albedo (0.6) surface has a set value of 0.01 for m, while m varies as shown for the 0.3 albedo surface. It is apparent that only a moderate amount of moisture ($m = 0.2$ producing a Bowen ratio near 1) is needed to significantly weaken any circulation tendencies arising from albedo differences between adjacent surfaces.

The results of Fig. 13a suggest that a significant circulation will still arise with a value of 0.05 for m, whereas the three-dimensional simulation of Mahrer and Pielke (1978) produced no circulation effects across adjacent surfaces taking m values of 0.0 and 0.05, and albedo values of 0.4 and 0.2. This apparent contradiction can be explained when the soil thermal properties are taken into account. The experiments of Fig. 13a were carried out using the sand properties (low conductivity of 0.31 W m^{-1} K^{-1}) for both soils. When the same experiments were done using the higher conductivity (2.57 W m^{-1} K^{-1}) salt properties, the re-

TABLE 2. Maximum values for runs 3, 4, 5 of east–west wind component u (cm s^{-1}), vertical velocity w (cm s^{-1}), and potential temperature difference $\Delta\theta$ (K) between mixed layers over sand and salt surfaces. All values are for cross-section AA′ (see Fig. 7a). Experiment denoted by "both" refers to run 3 in which differences in albedo and soil thermal properties were both modeled.

	Time (LST)														
	1000			1200			1400			1600			1800		
	u	w	$\Delta\theta$	u	w	$\Delta\theta$	u	w	$\Delta\theta$	u	w	$\Delta\theta$	u	w	$\Delta\theta$
Thermal properties difference	45	0.4	0.6	129	1.5	0.8	168	2.4	0.7	161	2.2	0.5	119	1.0	0.3
Albedo difference	40	0.3	0.5	121	1.5	0.8	197	3.1	0.8	247	4.1	0.9	359	3.5	0.8
Both	59	0.5	0.8	200	2.4	1.3	292	4.6	1.3	313	5.0	1.3	357	3.9	1.1

sulting differences in heat input were weaker. We have also done these experiments using the soil properties of Mahrer and Pielke (1978), which included the exceptionally high values of 5.86 W m^{-1} K^{-1} and 3.0 m^2 s^{-1} $\times$ 10^{-6} for conductivity and diffusivity. For comparison purposes, with m = 0.05 the heat input differences by 1700 LST for sand, salt, and Mahrer and Pielke soils, respectively, were 739, 498, and 437 W m^{-2}. These results reflect the fact that when more heat is being transferred to the soil, there is less available for sensible and latent heat fluxes.

The results of varying the moisture content of a relatively low-conductivity soil adjacent to a high-conductivity soil with m = 0.01 are shown in Fig. 13b. The albedo of both soils is 0.3. As with the albedo-induced circulations, the intensity is sharply reduced by the addition of moisture to the warmer surface. For a Bowen ratio of about 1 (m = 0.2), circulation effects are negligible. In reality, the addition of moisture to a soil will increase its ability to conduct heat and so the reductions in circulation are likely to be even greater than implied in Fig. 13b.

5. Discussion

Numerical model simulations and some observations have suggested that a dry salt lake of the order of 60–80 km across is capable of generating a mesoscale circulation that can significantly perturb the synoptic wind field up to at least 200 km from the lakeshore. Such perturbations may exert a strong influence on regional climate in areas of inland Australia, where a number of salt lakes of the above dimensions can be found. As discussed by Anthes (1984) though, the vertical motion fields associated with the circulation will only initiate or enhance rainfall in a convectively unstable environment with sufficient moisture. Inspection of cloud and rainfall records for stations in the salt-lake region of South Australia indicates that this type of situation occurs regularly, although a detailed frequency analysis has not been carried out. Thus the possibility of enhanced rainfall exists, although we have established no link in our investigation. Observations at The Salt Lake too have shown peripheral daytime cloud development during periods of relatively moist easterly flow.

In the previous section, mention was made of the similarity of our model circulations to observations of deeply penetrating disturbances generated at the coastlines of northeastern Australia. The most well-known of these is the "Morning Glory," a family of solitary waves manifesting itself as a series of roll clouds in the early daylight hours in western Queensland. These waves evolve at the leading edge of an internal bore generated further eastward around midnight by the collision of sea breezes from opposite coastlines of a 500 km wide peninsula (Clarke et al. 1981; Clarke 1984).

The majority of solitary waves observed in northern Australia near Tennant Creek by Christie et al. (1978) were attributed to deeply penetrating sea breezes from the coastline 500 km to the northeast or to the interaction of katabatic flow, from orography to the southeast, with the nocturnal inversion. However, a small number of waves were observed to propagate from the southwest where the only geographical feature of any note is Lake Mackay (salt), 600 km from Tennant Creek, and roughly 60 km in diameter. Our numerical results suggest that a salt lake of such dimensions can generate a deeply penetrating circulation, similar to the northeastern sea breezes that develop into solitary waves, and thus may be the source for the disturbances from the southwest. With a stronger following wind than used in section 4.2, such a disturbance can easily travel the required 600 km, as observed and modeled by Clarke (1984) for the Morning Glory. The propagation speed of about 15 m s^{-1} required for solitary waves to arrive at Tennant Creek in nocturnal hours, as observed, is well within the upper limit of 18 m s^{-1} measured by Christie et al. (1978).

While the study of solitary wave properties is a fascinating academic pursuit, it also has an important practical side related to aviation. Christie and Muirhead (1983a,b) discuss the intense transient horizontal and vertical wind-shear zones in the near-surface levels of these clear-air disturbances, stressing the hazard they represent to low-flying aircraft and recommending further studies be undertaken to identify regions of high solitary wave activity throughout Australia. We suggest the great salt lake area of central South Australia may be such a region.

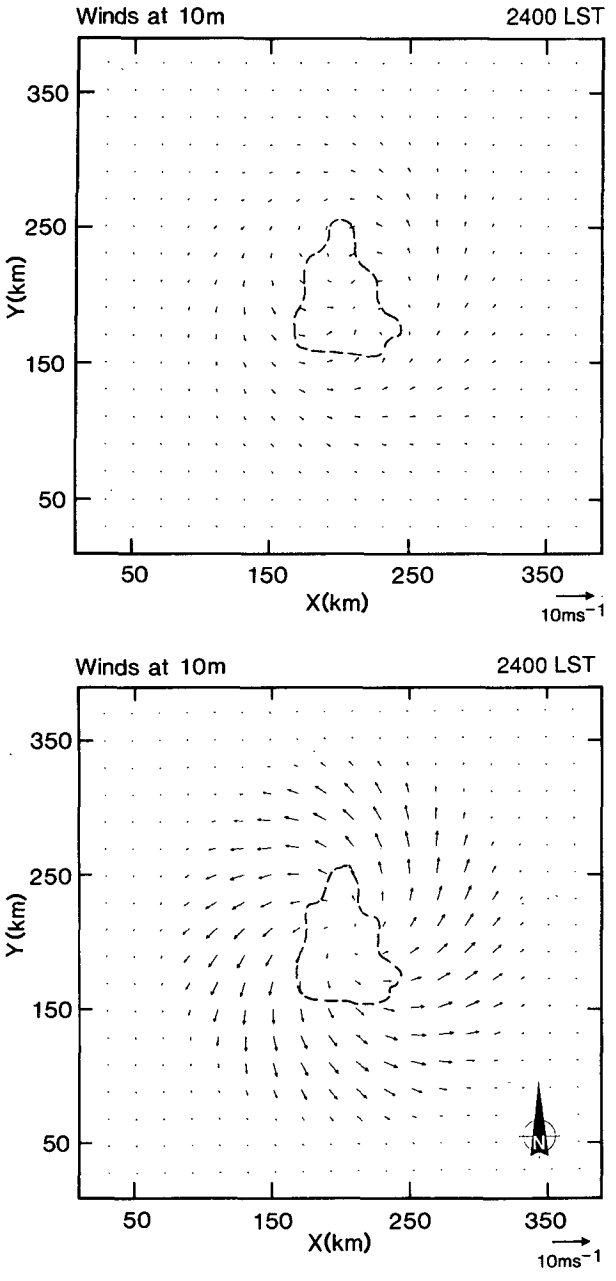

FIG. 11. Horizontal cross-section of winds at 10 m at 2400 LST for circulations induced by (a) differential soil thermal properties, and (b) albedo differential.

There are also important implications of this work in the wider area of drought research, particularly since the air motions that develop over salt lakes are partly controlled by albedo. In the years following the devastating Sahel drought of 1968–73, a vigorous debate began in the literature about the role of albedo change in drought persistence, the so-called "biogeophysical feedback mechanism." It was argued that a drought-induced reduction in plant cover and associated increase in albedo would result in a net-radiative loss, producing general subsidence and drying in an area, thereby inhibiting convection, cloud development, and rainfall, and enhancing the original decrease in plant cover (Otterman 1974, 1975; Charney 1975; Charney

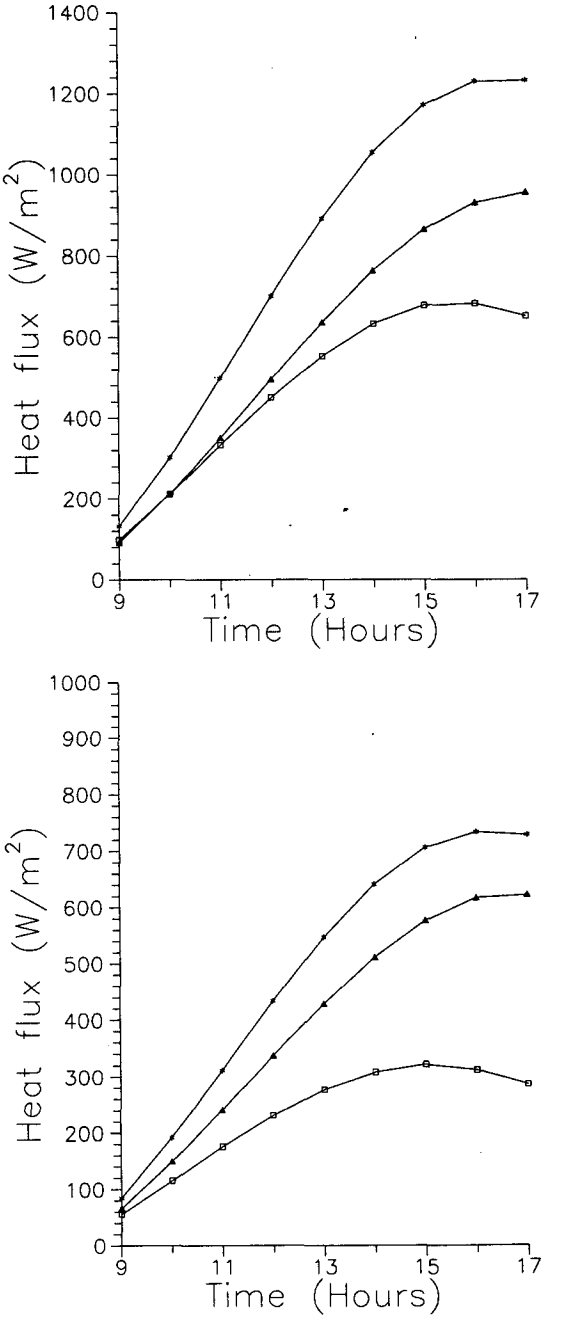

FIG. 12. Difference in time-integrated surface sensible heat flux over the sand and over the salt, as derived from one-dimensional experiments; (a) $m = 0.01$, (b) $m = 0.2$. Symbol * denotes case where both surfaces differ in albedo and soil properties (as in run 3); open square denotes case where only thermal properties differ (as in run 4); and triangle denotes case where only albedo differs (as in run 5).

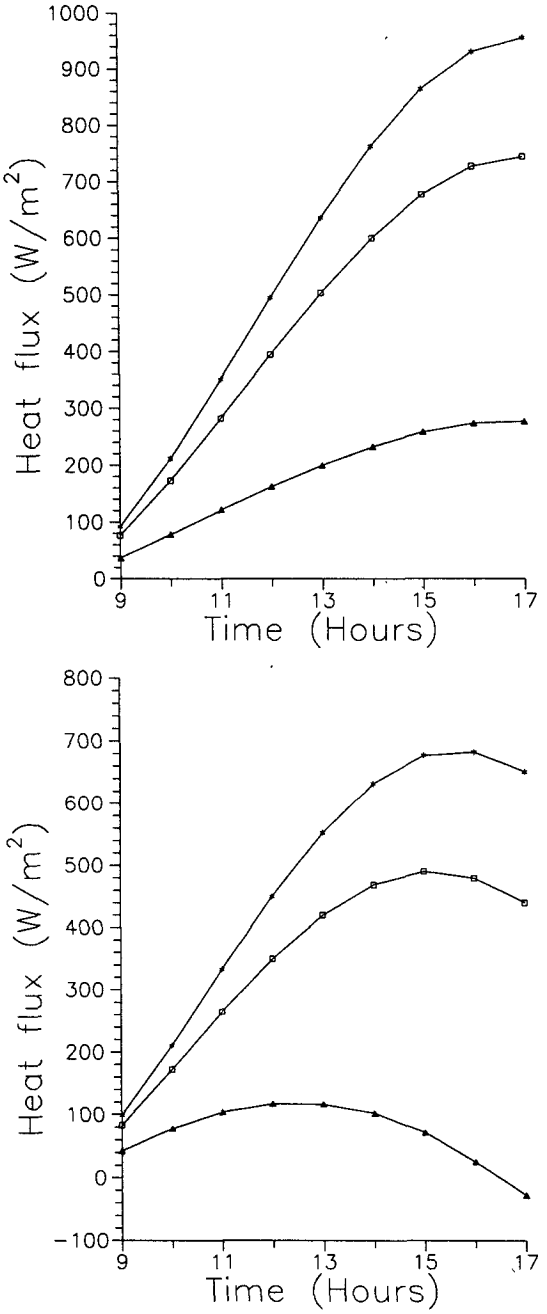

FIG. 13. Difference in time-integrated surface sensible heat flux over two surfaces, as derived from one-dimensional experiments; (a) surfaces have same soil properties (sand), but different albedos (0.6 and 0.3). Curves correspond to different values of m for 0.3 albedo surface. Here m remains constant at 0.01 for 0.6 albedo surface. (b) Surfaces have same albedo (0.3), but differ in soil properties. Parameter m varies as shown for lower conductivity surface and remains constant at 0.01 for higher conductivity surface. Symbol * denotes m = 0.01, open square denotes m = 0.05, and triangle denotes m = 0.02.

et al. 1977). Although this view had many detractors (Jackson and Idso 1975; Ripley 1976; Norton et al. 1979; Idso 1981), the debate has never been satisfactorily settled and we are clearly still a long way from a full understanding of the physical processes involved in desertification. Although it is recognized that a scale difference exists between the salt lakes studied in this paper and the larger areas of the world regularly affected by drought, our results suggest that albedo-induced mesoscale circulations on the margins of desert areas could have an important input to desertification processes.

Finally, a further environmental implication of these circulations is the possible modification of linear desert dunefields (Tapper 1990). Usually oriented parallel to the prevailing large-scale winds, these dunes show some perturbation around the larger Australian salt lakes (Wasson 1989, personal communication). Our numerical experiments suggest that salt-lake deformation of the regional windfield may be responsible.

6. Future work

The modeling results presented here confirm that a salt lake, completely devoid of surface water and lying in sand country of subdued relief is capable, by virtue of albedo and soil thermal characteristics alone, of generating a unique mesoscale thermal circulation. As such circulations may be very important in the regional climatology of large areas of inland Australia, future work will attempt to validate the model results over and downwind of one of the larger central Australian salt lakes. However, there are some areas where further work needs to be done on model input, particularly if more representative fluxes to the soil and to the atmosphere are to be incorporated. While we have used a value for the thermal conductivity of the salt crust (Table 1) that is consistent with the diurnal temperature wave observed beneath the surface, there is evidence to suggest that the thermodynamic behavior of the salt crust is quite different from the underlying saline sediments (Krusel 1988). Heat transfer through such nonuniform soils is still not fully understood (e.g., see Wiltshire 1983) and future field work will seek to improve specification of the crust and sediment characteristics. Further understanding of fluxes associated with such relatively small-scale features of the landscape as salt lakes is also important for larger-scale models, where a grid square can encompass more than one type of surface and where a representative area flux is required.

REFERENCES

Anthes, R. A., 1984: Enhancement of convective precipitation by mesoscale variations in vegetative covering in semi-arid regions. *J. Climate Appl. Meteor.*, **23**, 541–544.

Charney, J. G., 1975: Dynamics of deserts and droughts in the Sahel. *Quart. J. Roy. Meteor. Soc.*, **101**, 193–208.

——, W. J. Quirk, S. H. Chow and J. Kornfield, 1977: A comparative study of the effects of albedo change on drought in semi-arid regions. *J. Atmos. Sci.*, **34**, 1366–1385.

Christie, D. R., and K. J. Muirhead, 1983a: Solitary waves. A low-

level wind shear hazard to aviation. *Intern. J. Aviation Safety,* **1,** 169–190.

——, and ——, 1983b: Solitary waves: a hazard to aircraft operating at low altitudes. *Aust. Meteor. Mag.,* **31,** 97–109.

——, —— and A. L. Hales, 1978: On solitary waves in the atmosphere. *J. Atmos. Sci.,* **35,** 805–825.

Clarke, R. H., 1983: Fair weather nocturnal inland wind surges and atmospheric bores. Part I: Nocturnal wind surges. *Aust. Meteor. Mag.,* **31,** 133–145.

——, 1984: Colliding sea breezes and the creation of internal atmospheric bore waves: two-dimensional numerical studies. *Aust. Meteor. Mag.,* **32,** 207–226.

——, R. K. Smith and D. G. Reid, 1981: The morning glory of the Gulf of Carpentaria: an atmospheric undular bore. *Mon. Wea. Rev.,* **109,** 1729–1750.

Idso, S. B., 1981: Surface energy balance and the genesis of deserts. *Arch. Meteor. Geoph. Biokl. Ser. A.,* **30,** 253–260.

Jackson, R. D., and S. B. Idso, 1975: Surface albedo and desertification. *Science,* **189,** 1012–1013.

Krusel, N., 1988: Surface temperature—a case study at The Salt Lake, New South Wales. M.S. thesis, Department of Geography and Environmental Science, Monash University, 274 pp. [Available from the author at Dept. of Geography and Environmental Science, Monash University, Clayton, Victoria 3168, Australia.]

Lyons, W. A., 1972: The climatology and prediction of the Chicago lake breeze. *J. Appl. Meteor.,* **11,** 1259–1270.

McNider, R. T., and R. A. Pielke, 1981: Diurnal boundary layer development over sloping terrain. *J. Atmos. Sci.,* **38,** 2198–2212.

Mahfouf, J-F., E. Richard and P. Mascart, 1987: The influence of soil and vegetation on the development of mesoscale circulations. *J. Climate Appl. Meteor.,* **26,** 1483–1495.

Mahrer, Y., and R. A. Pielke, 1977: A numerical study of the airflow over irregular terrain. *Beitr. Phys. Atmos.,* **50,** 98–113.

——, and ——, 1978: The meteorological effect of the changes in surface albedo and moisture. *Israel Meteor. Res. Paper, Israel Meteor. Soc.,* **2,** 55–70.

Norton, C. C., R. F. Mosher and B. Hinton, 1979: An investigation of surface albedo variations during the recent Sahel drought. *J. Appl. Meteor.,* **18,** 1252–1262.

Oke, T. R., 1987: *Boundary Layer Climates.* 2nd edition, Methuen, London, 435 pp.

Ookouchi, Y., M. Segal, R. C. Kessler and R. A. Pielke, 1984: Evaluation of soil moisture effects on the generation and modification of mesoscale circulations. *Mon. Wea. Rev.,* **112,** 2281–2292.

Otterman, J., 1974: Baring high-albedo soils by overgrazing: a hypothesized desertification mechanism. *Science,* **186,** 531–533.

——, 1975: Reply to Jackson, R. D. and S. B. Idso. Surface albedo and desertification. *Science,* **189,** 1013–1015.

Pearson, R. A., 1973: Properties of the sea breeze front as shown by a numerical model. *J. Atmos. Sci.,* **30,** 1050–1060.

Physick, W. L., 1976: A numerical model of the sea-breeze phenomenon over a lake or gulf. *J. Atmos. Sci.,* **33,** 2107–2135.

——, and R. K. Smith, 1985: Observations and dynamics of sea breezes in northern Australia. *Aust. Meteor. Mag.,* **33,** 51–63.

Ripley, E. A., 1976: Drought in the Sahara: insufficient biogeophysical feedback? *Science,* **191,** 100.

Segal, M., R. Avissar, M. C. McCumber and R. A. Pielke, 1988: Evaluation of vegetation effects on the generation and modification of mesoscale circulations. *J. Atmos. Sci.,* **45,** 2268–2292.

Strong, A. E., 1972: The influence of a Great Lake anticyclone on the atmospheric circulation. *J. Appl. Meteor.,* **11,** 598–612.

Tapper, N. J., 1988: Some evidence for a mesoscale thermal circulation at The Salt Lake, New South Wales. *Aust. Meteor. Mag.,* **36,** 101–102.

——, 1990: Evidence for a mesoscale thermal circulation over dry salt lakes. *Palaeogeog. Palaeoclim. Palaeoecol.,* in press.

Wiltshire, R. J., 1983: Periodic heat conduction in a non-uniform soil. *Earth. Surf. Processes Landforms,* **8,** 547–555.

Yan, H., and R. A. Anthes, 1988: The effect of variations in surface moisture on mesoscale circulations. *Mon. Wea. Rev.,* **116,** 192–208.